Coupled Climate Modelling at GFDL: Recent Accomplishments and Future Plans

Thomas L. Delworth[1], Anthony J. Broccoli[1], Keith Dixon[1], Isaac Held[1], Thomas R. Knutson[1], Paul J. Kushner[1], Michael J. Spelman[1], Ronald J. Stouffer[1], Konstantin Y. Vinnikov[2], and Richard E. Wetherald[1]

[1]GFDL/NOAA P.O. Box 308, Princeton University, Princeton, NJ 08542 USA
[2]Department of Meteorology, University of Maryland, College Park, MD 20742 USA

corresponding e-mail: td@gfdl.gov

1. Introduction and description of GFDL coupled climate models

Coupled ocean-atmosphere models have been used extensively at GFDL over the past several decades for a wide variety of climate modelling studies. These include pioneering studies of the transient response of the climate system to increasing greenhouse gas concentrations, as well as studies of paleoclimate and internal variability of the coupled ocean-atmosphere-land system.

Continuing in this tradition, there are currently two distinct coupled ocean-atmosphere climate models in use at GFDL for research on global warming and other aspects of climatic sensitivity and variability. The models differ in resolution by a factor of approximately 2 but share similar physics. The R30 coupled model, which has been under development for several years, is now being used for the generation of global warming scenarios and studies of decadal-to-centennial climatic variability. This model has an atmospheric horizontal resolution of 3.75° longitude and 2.25° latitude, with 14 levels in the vertical. It is coupled to an ocean model with an approximately 2° horizontal resolution, a simple current-drift sea-ice model, and a "bucket" land model. Flux adjustments are incorporated to reduce climate drift and facilitate the simulation of a realistic mean state. The atmospheric component of this model has been studied extensively. Analyses of a large ensemble of 40-year experiments with prescribed observed sea surface temperatures (SSTs) show a highly realistic response of the model to tropical Pacific SST variations, as well as realistic representations of mid-latitude variability. Selected output from the R30 atmospheric model is available at "*http://www.cdc.noaa.gov/gfdl/index.shtml*". The R15 coupled model has similar physics but lower spatial resolution.

Several long control integrations have recently been performed, exceeding 1000 years for the R30 model and 12,000 years for the R15 model. A variety of experiments with greenhouse gas and sulphate aerosol forcings has also been conducted. The principal scientific findings from our recent modelling studies related to global warming are summarized below.

2. Simulation of the climate of the 20th and 21st centuries

A major recent activity has been the use of the R30 coupled model to study climate change over the 20th and 21st centuries. A suite of five simulations over the period 1865-2089 has been completed, in which the model is forced with estimates of the observed and projected effective greenhouse gas concentrations and sulphate aerosols. An equivalent CO_2 concentration is used to represent changes in all of the trace greenhouse gases, and changes in aerosol loading are modelled by altering the surface albedo (Mitchell et al., 1995; Haywood et al., 1997). The runs proceed until the late 21st century with equivalent CO_2 increasing at the rate of 1% per year after 1990. The ensemble members differ in their initial conditions, which are taken from widely separated points in the long control run. In addition, a suite of six integrations is currently underway using new scenarios proposed by IPCC-2000 (scenarios A2 and B2).

Shown in Fig. 1 (page 20) is the time series of observed global mean surface temperature (thick, black line), as well as the time series simulated from the five members of the R30 ensemble (various coloured lines). The observed temperature record of the 20th century is characterized by an overall warming trend, largely occurring in two distinct periods (1925-1944, and the late 1970s to the present). The ensemble members largely capture the amplitude and timing of the 20th century warming. The simulated time series form a spread around the observed record, thereby offering a perspective on the role of internal variability. Since each model starts from independent initial conditions, the internal variability realized in each of the ensemble members is independent. Closer examination of the time series for the individual realizations, however, reveals that one of the

ensemble members (Experiment 3) appears to track the observed time series quite closely, including the observed warming of the 1920s and 1930s. Since the members differ only in their realizations of internal variability, this suggests that internal variability may have played an important role in the observed warming of the 1920s and 1930s.

The equilibrium response of this model to a doubling of greenhouse gas concentrations is 3.4K, approximately in the middle of the 2.1K to 4.6K range cited in IPCC (table 6.3, Kattenberg et al., 1995). The agreement between the model and observed trends suggests that this level of climate sensitivity cannot be excluded based upon the observational record.

The geographical distribution of simulated surface temperature trends has been compared with the observed trends for the period 1949-1997 (Knutson et al.,1999). The simulated and observed trends are consistent in most regions, taking into account the internal variability of the trends, as estimated from the model. There are also several areas which are inconsistent, all of which are regions where substantial cooling has been observed (primarily the midlatitude North Pacific, and parts of the Southwest Pacific and the Northwest Atlantic). These regional inconsistencies are very likely the result of deficiencies in one or more of the following: 1) the prescribed radiative forcing; 2) the simulated response to this forcing; 3) the simulation of internal climatic variability; and 4) the observed temperature record. Distinguishing between these alternatives is a high priority for future research.

The observed temperature trends in this same period have also been compared to trends generated by internal climate variability in the control integration. In nearly 50% of the areas analysed (where data was deemed adequate for this purpose), the observed warming trends exceed the 95th percentile of the simulated distribution of internally generated trends for the same location. If the model's simulation of internal climate variability is accurate, these observed trends are very unlikely to have occurred due to internal dynamics of the climate system.

Studies have also focused on changes in the large-scale extratropical atmospheric circulation under greenhouse warming. Differing responses were found in the two hemispheres. The SH tropospheric response consists of a summertime poleward shift of the westerly jet, the storm tracks, and the atmospheric and oceanic mean meridional overturning. The simulated signal emerges robustly early in the next century when compared to the control run. The signal-to-noise ratio, however, is relatively small because the signal projects strongly and positively onto the model's Antarctic Oscillation (AAO) pattern. (The AAO and its NH counterpart, the Arctic Oscillation (AO), are the principal modes of variability of the extratropical zonal-mean circulation.) The positive sign of the projection is in agreement with observed trends.

In contrast with the SH, the NH tropospheric circulation response involves an equatorward jet shift, an enhanced Aleutian Low, and a negative sea-level pressure anomaly over the Arctic. The response in the Aleutian Low and the Arctic SLP agree in sign, but not in magnitude, with recent observed trends. In particular, the observations show a much larger negative trend in Arctic SLP than is seen in the simulations. We are currently exploring the factors that underlie this discrepancy.

3. Continuing studies with the R15 Coupled Model

The speed of the R15 coupled model has allowed a wide range of recent studies with this model. These studies have focused on both radiatively forced climate change and internal variability of the coupled ocean-atmosphere system. Some examples of recent studies are highlighted below.

a. Large ensemble of climate change simulations

Dixon and Lanzante (1999) have recently conducted a nine member ensemble of greenhouse gas plus sulphate aerosol experiments covering the period 1765 to 2065. The study found a relatively small sensitivity of simulated surface air temperature to the year in which the model integration started (1765, 1865, or 1915). This result provided the rationale for starting the R30 experiments at year 1865. The ensemble of experiments was also used to assess uncertainties in various aspects of climate change, including global mean temperature response and the thermohaline circulation (THC). The mechanisms responsible for the simulated weakening of the THC were further investigated in Dixon et al. (1999) who showed that enhanced atmospheric water flux convergence was the primary factor leading to a reduction of the simulated THC. Additional analyses are also being conducted on the hydrologic cycle and its response to greenhouse warming, with emphasis on the near-surface continental climate (Wetherald and Manabe, 1999).

b. Sea ice and climate change

Vinnikov et al. (1999) compared the simulated decrease of Arctic sea ice in the GFDL R15 model to the observed decrease. The results (Fig. 2, page 20) demonstrate a remarkable agreement between simulated and observed trends. Further, they demonstrated that the observed decrease in sea ice extent is outside the range of internal variability of the model. Additional analyses using the R30 model provide generally similar results.

Analyses are ongoing to assess Southern Hemisphere sea ice changes, as well as changes in snow cover.

c. Multidecadal variability

Delworth and Mann (2000) have recently compared the simulated multidecadal variability in the North Atlantic of the R15 coupled model to a new multiproxy reconstruction of climate over the last several centuries. In both the model and proxy reconstructions the spectrum of climate variability has a clear peak on the multidecadal time scale (approximately 60-80 years). The simulated variability involves fluctuations in the North Atlantic THC. A comparison of the spatial structures between the model and the observations reveals relatively good agreement in the North Atlantic sector. Preliminary analyses with the R30 coupled model indicate that similar variability exists in the higher resolution model. Such detailed comparisons of model and proxy data offer a promising pathway for increasing our understanding of decadal to centennial scale variability. Delworth and Greatbatch (2000) have also used the R15 model to demonstrate that such multidecadal variability of the THC is partially attributable to stochastic forcing of the ocean through the surface heat flux.

d. Extreme event in a 12,000 year coupled run

A control integration of one version of the R15 coupled model now has been extended beyond 12,000 years, thereby offering insights into centennial to millennial scales of variability. In this extended run a highly anomalous event occurs in the high latitudes of the North Atlantic at approximately model year 3100. A large pulse of fresh water, originating in the Arctic, moves southward through the Fram Strait into the North Atlantic. This fresh water pulse is accompanied by reduced oceanic convection and cold surface air temperature (annual mean anomalies of -4 K, corresponding to 6 standard deviations below the mean). This event appears to be an extremely high amplitude realization of a prominent mode of internal variability of the coupled system (Delworth et al., 1997). Investigations of the dynamics of this variability are ongoing.

4. Simulation of the Ice Age - implications for climate sensitivity

A major source of uncertainty in climate model projections of future climate involves the sensitivity of the climate system to radiative forcing. One way to evaluate the realism of a model's climate sensitivity is to simulate climates of the distant past where sufficient evidence exists to estimate the changes in climate forcing and response. In pursuit of this goal, Broccoli (2000) used a atmosphere-mixed layer ocean model, whose atmospheric component is nearly identical to the one employed in the R30 coupled model, to examine the changes in tropical climate induced by the relatively well-documented changes in radiative forcing that occurred 21,000 years ago during the last glacial maximum. At this time, continental ice sheets were greatly expanded, atmospheric CO_2 was reduced by approximately 25%, and sea level was more than 100 m lower. When incorporated into the climate model, these changes produced a mean cooling of 2 K for the region from 30°S to 30°N.

Comparison of this simulated cooling with a variety of paleodata indicates that the overall tropical cooling is comparable to paleoceanographic reconstructions based on alkenones and species abundances of planktonic microorganisms, but smaller than the cooling inferred from noble gases in aquifers, pollen, snow line depression, and the isotopic composition of corals. The paucity of paleoclimatic evidence for tropical cooling smaller than that simulated by the model suggests that it is unlikely that the model exaggerates the actual climate sensitivity in the tropics. A more definitive evaluation of the realism of the tropical sensitivity of the model must await the resolution of the differences in the magnitude of tropical cooling reconstructed from the various paleoclimatic proxies.

5. Future plans

A major reorganization of the model development activity is underway at GFDL. The new modelling system will consist of both a software infrastructure that is shared across models and specific models that are constructed on top of this infrastructure, including fully coupled climate models. The latest version of GFDL's Modular Ocean Model will be incorporated into this system along with new land and sea-ice models under development. Two distinct atmospheric dynamical cores are included in the current realization of this system: a grid-point model on the B-grid, and a standard spectral model with the option of grid advection of water vapour and other tracers. A variety of improvements to the atmospheric physics are under active development, including a new radiative transfer code, boundary layer parameterisations, convective closures and cloud prediction schemes with prognostic cloud water. The hope is that this new structure will reduce the time required to develop new coupled models, ease the transition to new computer architectures, provide for more integrated research activities within the lab, and foster more extensive extramural collaborations. Research on seasonal-to-interannual forecasting and on the circulation of the middle atmosphere, which are currently conducted with models that are distinct in many different ways from the climate model, will be using the same modelling system

and sharing most physics modules with future climate models.

The development of a new climate model for use in long control integrations, global warming scenario generation, and paleoclimatic studies is currently focused on a T42 resolution spectral atmosphere coupled to an ocean model with 2° horizontal resolution, except in the tropics where finer resolution is retained to provide a better ENSO simulation. An ice model with viscous-plastic rheology will also be incorporated. A 1° version of the ocean model is also undergoing initial testing. At present, the oceanic, land, and ice components are closer to being finalized than the atmospheric component. Plans also involve using both grid and spectral atmospheric models, at resolutions of T106 and higher, coupled to mixed layers or with fixed SSTs (or SSTs generated in lower resolution coupled model global warming scenario studies) to evaluate how alternative atmospheric physical packages affect climate sensitivity and regional climate change.

References

Broccoli, A.J., 2000: Tropical cooling at the last glacial maximum: An atmosphere-mixed layer ocean model simulation. *J. Climate*, in press.

Chapman, W.L., and J.E. Walsh, 1993: Recent variations of sea ice and air temperature in high latitudes. *Bull. Amer. Meteor. Soc.*, **74**, 33-47.

Delworth, T.L., S. Manabe, and R.J. Stouffer, 1997: Multidecadal climate variability in the Greenland Sea and surrounding regions: a coupled model simulation. *Geophys. Res. Lett.*, **24**, 257-260.

Delworth, T.L., and M.E. Mann, 2000: Observed and simulated multidecadal variability in the Northern Hemisphere. *Climate Dynamics*, accepted.

Delworth,T.L., and R.E. Greatbatch, 2000: Multidecadal thermohaline circulation variability driven by atmospheric surface flux forcing, *J. Climate*, in press.

Dixon, K.W., and J. Lanzante, 1999: Global mean surface air temperature and North Atlantic overturning in a coupled GCM climate change experiment. *Geophys. Res. Lett.*, **26**, 2749-2752.

Dixon, K.W., T.L. Delworth, M. Spelman, and R.J. Stouffer,1999: The influence of transient surface fluxes on North Atlantic overturning in a suite of coupled GCM climate change experiments. *Geophys. Res. Lett.*, **26**, 1885-1888.

Haywood, J.M., R.J. Stouffer, R.T. Wetherald, S. Manabe, and V. Ramaswamy,1997: Transient response of a coupled model to estimated changes in greenhouse gas and sulfate concentrations. *Geophys. Res. Lett.*, **24**, 1335.

Jones, P.D., 1994: Hemispheric surface air temperature variations: a reanalysis and an update to 1993. *J. Climate*, **7**, 1794-1802.

Kattenberg, A., *et al.* in *Climate Change 1995: The Science of Climate Change* (eds. J. Houghton et al.) 285-357 (Cambridge Univ. Press, 1996).

Knutson, T.R., T.L. Delworth, K.W. Dixon, and R.J. Stouffer, 1999: Model assessment of regional surface temperature trends (1949-97). *J. Geophys. Res.*, in press.

Mitchell, J.F.B., T.C. Johns, J.M. Gregory, S.F.B. Tett, 1995: Climate response to increasing levels of greenhouse gases and sulfate aerosols. *Nature*, **376**, 501.

Parker, D.E., C.K. Folland, and M. Jackson, 1995: Marine surface temperature: observed variations and data requirements. *Clim. Change*, **31**, 559-600.

Robinson, D. A., 1993: Hemispheric snow cover from satellites. *Ann. Glaciol.*, **17**, 367-371.

Vinnikov, K.Y., A. Robock, R.J. Stouffer, J.E. Walsh, C.L. Parkinson, D.J. Cavalieri, J.F.B. Mitchell, D. Garrett, and V.F. Zakharov, 1999: Detection and attribution of global warming using Northern Hemisphere sea ice. *Science*, in press.

Wetherald,R.E., and S. Manabe, 1999: Detectability of summer dryness caused by greenhouse warming. *Climatic Change*, **43**, 495-511.

Plate 1: Figures from Sperber et al. (see page 4)

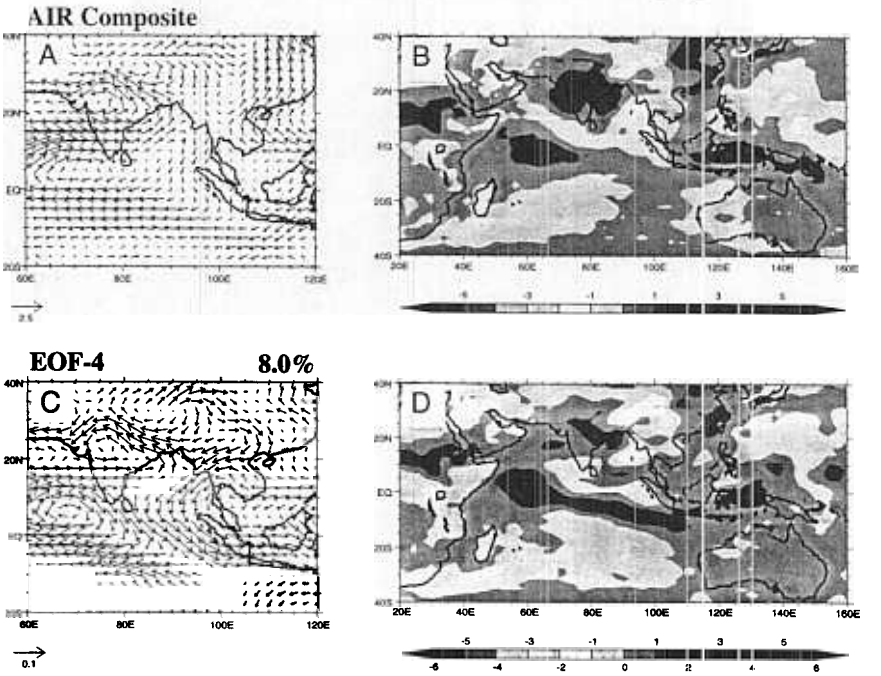

Fig. 2: The composite difference of seasonally averaged (a) 850hPa wind (unit vector=2.5ms^{-1}) and (b) precipitation anomalies (mm day^{-1}) for years of above normal all-India rainfall versus years of below normal all-India rainfall (see Fig. 1). (c) The fourth mode of variability extracted from an empirical orthogonal function analysis of seasonal anomalies of 850hPa wind. The magnitude of the wind anomalies is the product of the principal component time series and the components of the wind. Typical variations of this mode are 1-2ms^{-1}. (d) precipitation anomalies (mm day-1) constructed from the difference of composites based on years when the principal component time series of mode 4 was of above normal versus below normal using +/-0.5 standard deviations thresholds.

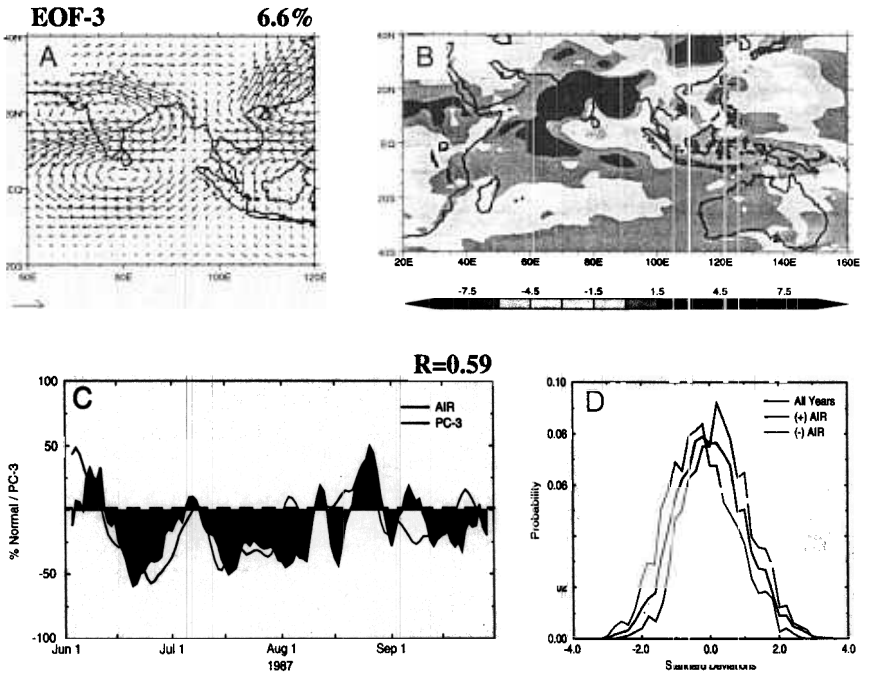

Fig. 3: (a) The third mode of variability extracted from an empirical orthogonal function analysis of daily anomalies of 850hPa wind. Typical variations of this mode are 2-4ms^{-1}. (b) precipitation anomalies (mm day^{-1}) constructed from the difference of composites based on days when the principal component of mode 3 was of above normal versus below normal using +/-1 standard deviations thresholds. (c) Observed daily all-India rainfall (filled curve, expressed as a percentage of normal) and the principal component time series of mode 3 (red line) for 1987. Both time series have been smoothed with a 5-day running mean. (d) Probability distribution functions of the principal component time series of mode 3 for all years (black line), years of above normal all-India rainfall (green line) and below normal all-India rainfall (red line). The years of above normal and below normal all-India rainfall are given in Fig. 1.

Plate 2: Figures from Delworth et al. (see page 15)

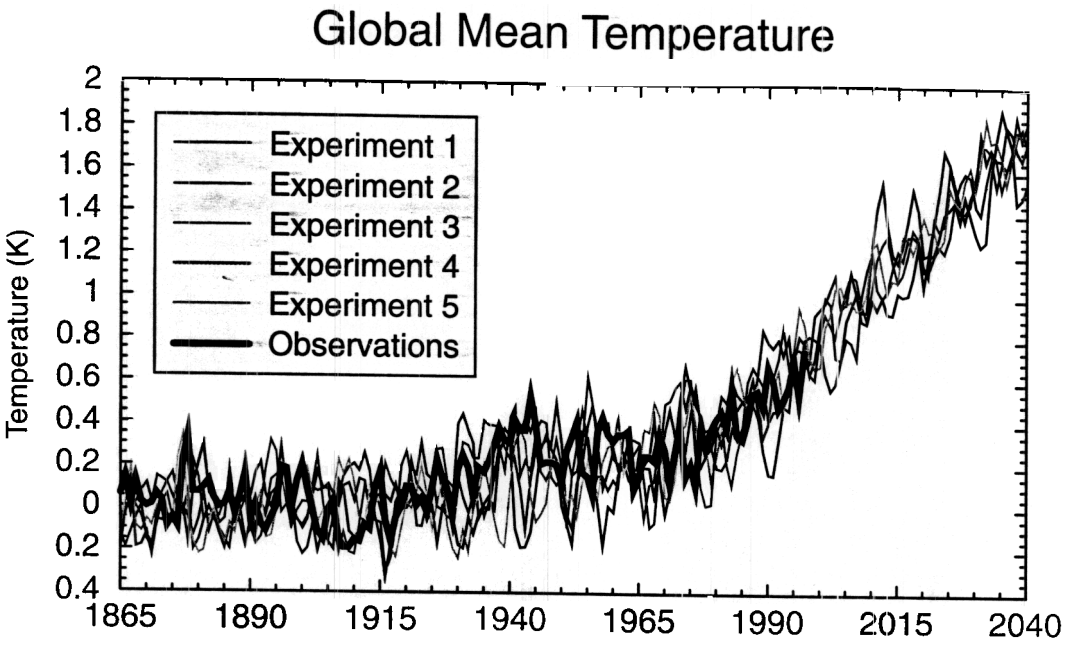

Fig. 1: Time series of observed (heavy black line) and simulated (various thin colored lines) global mean surface temperature over the period 1865 to 2040 (1997 for the observations). The simulated lines are from 5 independent realizations of the GFDL R30 coupled model forced with estimates of observed greenhouse gases and sulfate aerosols until 1990, and projections thereafter. The model output is sampled only for those locations and times at which observational data exist. For both model and observations, surface air temperature is used over the continents, while sea surface temperature is used over the oceans. The observed data are a combination of the Jones (1994) surface air temperature data and the Parker et al. (1995) sea surface temperature, updated through 1997. Anomalies are plotted relative to the 1880-1920 mean for both the model and observations.

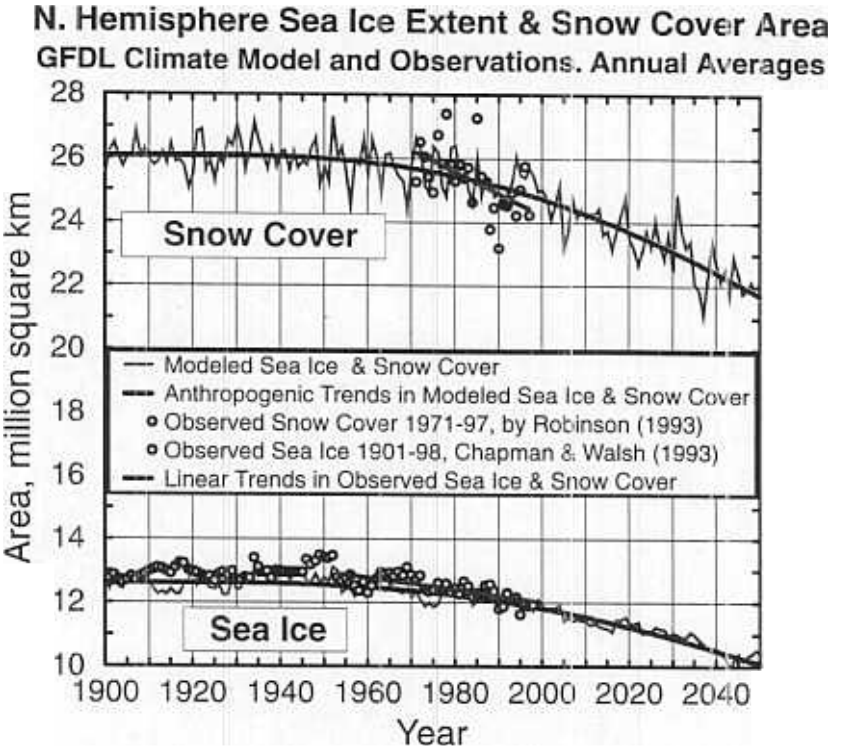

Fig. 2: Observed and simulated time series of Northern Hemisphere sea ice extent and snow cover (after Vinnikov et al.,1999).